Understanding non-classical tipping: rate-induced tipping and novel 'reverse' tipping phenomena in a nonautonomous spatially extended system

Anne Marie Warren

Submitted under the supervision of Dr. Arnd Scheel to the University Honors Program at the University of Minnesota-Twin Cities in partial fulfillment of the requirements for the degree of Bachelor of Science, *summa cum laude* in Mathematics.

May 13, 2025

Acknowledgments

I would like to extend my heartfelt thanks to the following people, whose impacts on the completion of this thesis, and my broader academic career, are indelible.

To my excellent advisor, Dr. Arnd Scheel, for your constant guidance and encouragement. From humble beginnings in a first course in differential equations, through this thesis, the culmination of my undergraduate career, your mentorship has been integral to my academic development. I owe my skill and confidence in research mathematics principally to you.

I am duly grateful to the members of my thesis committee, Dr. Richard McGehee and Dr. Markus Keel.

> To Dr. McGehee– you inspire me to keep my passions and interests close to my work in mathematics, and serve as a shining example that that is possible.
>
> To Dr. Keel– one of the most dynamic lecturers I've had the pleasure of learning from. You challenge and inspire me to to hold onto my excitement and love for the subject, and pass on that love to those who will come after me.

In time in the School of Mathematics at the University of Minnesota, I have truly had nothing but positive experiences with my professors, classmates, friends, and colleagues. Thank you to all of those who have colored my undergraduate career. I cannot possibly name you all.

Finally, to my family– my mother Henriette, my father Jeremy, my sister Elsie, my grandparents, I am forever grateful for your constant support, love, and encouragement. None of this would be possible without you. I love you to infinity and beyond.

Contents

Introduction

Complex systems are susceptible to sudden changes in state; this change may be merely a transient effect, or can be the result of a complete loss in equilibrium stability. Such 'tipping' events– these dramatic changes in system state– can range from benign to catastrophic, and may not, in general, be reversible. Because of this, understanding the nature of 'tipping' in dynamical systems is critical to characterizing many systems of interest; particularly with respect to models of the global climate, tipping represents regime changes that may be irreversible. The far-reaching implications of such an event make identifying different modes of tipping and developing the ability to predict them before criticality of great interest [2], [4], [10], [19].

Tipping as a direct result of a bifurcation is a well studied problem, having been a rich field of mathematical study since the idea of a 'bifurcation' was introduced by Poincaré in 1885 [16]. Several other tipping modes have been identified, e.g. noise-induced [5] or rate-induced tipping [6], [22], which arise from distinctly different mechanisms. In particular, theories of rate-induced tipping present a valuable framework for understanding critical points in systems with rapidly changing parameters. As global average temperatures rise, it seems equally plausible to ask if there might exist a critical *rate* of warming which triggers a catastrophic shift in global climate, as it does to ask if there might exist a critical temperature *value*. Many other systems exist where bifurcation-induced tipping alone may fail to fully account for qualitative phenomena of interest.

Chapter 1 of this work focuses on rate-induced tipping, compiling the existing theory of rate-induced tipping (section 1.1), current understanding of its interactions with the aforementioned bifurcation- and noise-induced tipping mechanisms (section 1.2), and exploring its applications (section 1.3). Chapter 2 explores the novel 'reverse' tipping phenomenon which arises in a spatially extended system where rate-induced tipping is also exhibited. This mechanism allows a tipping front to propagate *ahead* of a traveling 'trigger' front. For an effect with a tipping profile (some spatially dependent and traveling object which causes tipping in its wake), we observe, under certain conditions tied to the speed of the tipping profile's propagation, that a 'runaway' tipping effect can be triggered. This runaway effect results in a new tipping front propagating ahead of the original tipping front, so that even in areas expected to be unaffected by the tipping front, loss of stability, change in state, and tipping may occur. This phenomenon is reminiscent of a cascade effect, and its ability to propagate beyond expected boundaries and at higher speeds presents concerns in real-world models where the behavior might be present. We formally define the problem in section 2.1, and characterize this phenomenon in a relevant limiting regime (section 2.2). Discussion of the results and implications for future study can be found in section 2.3.

Chapter 1

Understanding rate-induced tipping

1.1 Current theory

In general, rate-induced tipping ('r-tipping') can be understood in nonautonomous systems as a failure of solutions initially near a moving attractor to track this attractor as it moves above a critical rate. This is distinct from bifurcation-induced tipping ('b-tipping'), which occurs at a certain critical parameter value, independent of rate, and under which there is a fundamental change in the stability of the system. In the moving-frame autonomous system, such 'b-tipping' can be characterized as a classical bifurcation of the moving stable state. In 'r-tipping,' however, the mechanism cannot be described as a classical bifurcation– the original attractor does *not* lose stability and persists despite the departure of solutions to a different regime.

For example[1], consider the following simple bi-stable system, that is shifted by a time dependent value u that in this case monotonically increases from 0 to 2 at some rate c.

$$x_t = (x-u) - (x-u)^3 \quad \text{where, e.g.} \quad u_t = cu(2-u) \tag{1.1}$$

For $u = 0$, the 'upper' and 'lower' equilibria (both saddles) are at $x = -1$ and $x = 1$ respectively, with a totally unstable equilibrium separating them at $x = 0$. As u approaches 2 (reaching it as $t \to +\infty$), the equilibria are accordingly shifted to $x = 1$, $x = 2$, and $x = 3$. As $t \to +\infty$, the question is whether solutions starting near the upper state track this equilibrium as it shifts, or tip to the lower stable state. Or, from the lens of opinion dynamics– suppose the two moving quasi-stable equilibria are the locations of two political parties. As they travel, they move along an axis of, say, opinion on a certain policy. Then solutions 'tracking' or 'tipping' from the leading QSE can be conceptualized as asking the following question: is there a rate of radicalization past which the more extreme party loses its members to the trailing one? It turns out there is such a $c_\star$, which can be analytically described by considering the behavior of the unstable manifold of the upper ($u = 0$, $x = 1$) equilibrium. At the critical rate $c_\star$, this unstable manifold has a nonempty intersection with the stable manifold of the middle ($u = 2$, $x = 2$) equilibrium. Above this rate, solutions converge to the lower stable equilibrium ($u = 2$, $x = 1$) as $t \to +\infty$, a tipping solution! The

[1] Credit for this illustration is due to my advisor, Dr. Arnd Scheel, and his lecture notes for a graduate course in differential equations at the University of Minnesota [18]

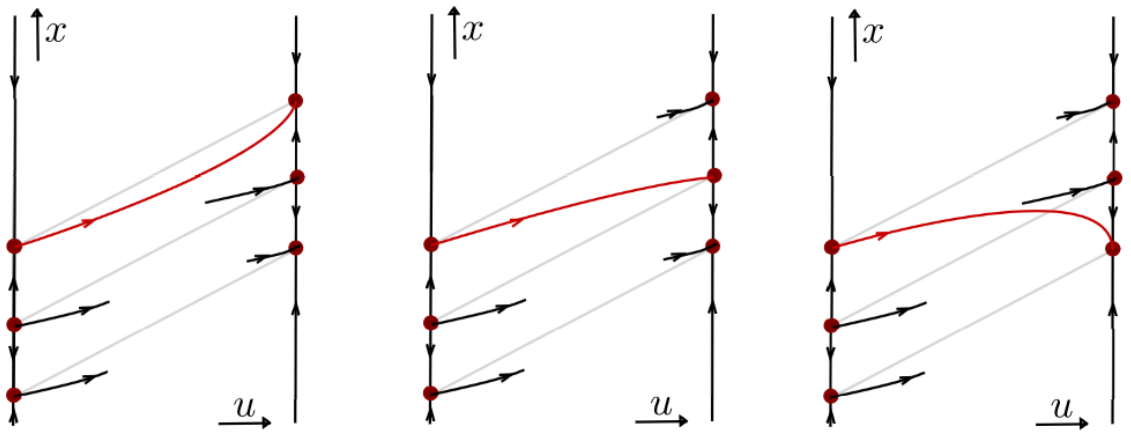

Figure 1.1: Heteroclinic orbits in the cases $c < c_\star$, $c = c_\star$, and $c > c_\star$ resp.

heteroclinic orbits in each of the cases $c < c_\star$, $c = c_\star$, and $c > c_\star$ (see fig. 1.1) illustrate this change.

Although this was an intentionally basic example, the characterization of rate-induced tipping as a qualitative change in heteroclinic orbits is a property seen, and exploited, in more complex or generalized systems.

Characterizing r-tipping from a broader perspective involves the development of general criteria for the presence or absence of such effects, as done by Ashwin et al. [2]. In the linear case, in a system of arbitrary dimension $x \in \mathbb{R}^n$, with a quasi-static equilibrium (QSE) $\tilde{x}(\lambda)$ and parameter λ, they define a 'tipping radius' $R > 0$ so that given an initial condition x_0 such that $|x_0 - \tilde{x}(\lambda)| < R$, x evolves according to

$$x_t = M(x - \tilde{x}(\lambda)), \quad |x - \tilde{x}(\lambda)| < R \tag{1.2}$$

with M some fixed stable linear operator. Incorporating time dependence of λ, this becomes

$$x_t = M(x(t) - \tilde{x}(\lambda(t))) \tag{1.3}$$

and the criterion for tipping is the existence of some t_0 such that $|x(t_0) - \tilde{x}(\lambda(t_0))| = R$. Then, in terms of the drift $r(t) = \tilde{x}_t$ of the QSE and the matrix norm $||M|| = \sup_{\nu \neq 0} \frac{|M\nu|}{|\nu|}$, assuming M invertible and $r \neq 0$, sufficient conditions for cases of r-tipping are

$$||M^{-1}|| \cdot |r| < R \ \text{(absence)} \qquad ||M||^{-1} \cdot |r| > R \ \text{(presence)} \tag{1.4}$$

for 'steady drift' (i.e. r constant). The conditions for avoiding r-tipping for a general $r(t)$ become

$$\frac{c}{\beta} r_{\max}(t) < R \tag{1.5}$$

for a choice of c, β such that $||e^{Mu}|| \leq ce^{-\beta u}$. This choice is possible from the assumption that M is stable, but in general is not straightforward unless M is scalar, in which case a choice of $c = 1$, $\beta = -M$ reduces eq. (1.5) to

$$||M^{-1}|| \cdot r_{\max}(t) < R. \tag{1.6}$$

Ashwin et al. then generalize this approach to nonlinear systems, so 'tipping radius' becomes an 'effective tipping radius,' which may not be directly analogous due to nonlinear effects and dependence on exact trajectory or shape of the QSE's local basin of attraction.

This work is rather naturally followed up by Ashwin, Perryman, and Wieczorek [1], which considers nonlinear systems

$$x_t = f(x, \Lambda(rt)) \tag{1.7}$$

with $x \in \mathbb{R}^n$, $t \in \mathbb{R}$, fixed rate $r > 0$, and sufficiently smooth functions $\Lambda \in C^2(\mathbb{R}, \mathbb{R}^d)$ and $f \in C^2(\mathbb{R}^{n+d}, \mathbb{R}^n)$. This general class of systems is reduced by the assumption that asymptotically the dynamics are autonomous, which allows the following analysis. In one dimension, and for Λ bounded (so $\lambda_- < \Lambda(rt) < \lambda_+$ for t finite) with $\Lambda(rt) \to \lambda_\pm$ for $t \to \pm\infty$, conditions for r-tipping are framed in terms of tracking stable paths, which are continuous curves

$$(X(rt), \Lambda(rt)) \to (X_\pm, \Lambda_\pm) \text{ for } t \to \pm\infty \tag{1.8}$$

such that their image lies within $\overline{\mathcal{X}}_{\text{stab}}$, the set of equilibria of the system which are linearly stable. The authors define two related notions of 'ε-close tracking' and a weaker 'endpoint tracking' of a solution $x(t)$ with respect to a stable path $(X(rt), \Lambda(rt))$ as

$$|x(t) - X(rt)| < \varepsilon \quad \forall t \in \mathbb{R} \tag{1.9}$$

and

$$\lim_{t \to \pm\infty} x(t) = X_\pm \quad \text{for } (X(rt), \Lambda(rt)) \to (X_\pm, \Lambda_\pm) \text{ as } t \to \pm\infty \tag{1.10}$$

respectively. These conditions are then used to define a property of stable path called 'forward basin stability,' which requires the basin of attraction of a stable equilibrium to contain the closure of the set of all possible earlier positions of X along the path. They are then able to prove a few useful criteria for r-tipping based on this property.

This idea of 'forward basin stability,' while definable in arbitrary dimensions, no longer necessarily determines the presence of r-tipping in dimensions higher than one. Kiers and Jones address this by defining a related condition called 'forward inflowing stability' which *can* guarantee sufficient conditions for the presence or absence of r-tipping in higher dimensional systems [8]. While forward basin stability is a property of equilibria along a path in relation to basins of attraction along the path, forward inflowing stability broadens this to the relation of these equilibria to forward invariant sets along the path. This approach, while providing valid criteria for 'r-tipping,' suffers from the difficulty of actually determining whether a given path is forward inflowing-stable.

Kuehn and Longo propose a more computationally favorable heuristic for r-tipping, building off similar ideas as those already discussed ([1], [8]), but focusing on approximation of solutions to estimate the presence or absence of tipping [9]. The general approach is asymptotic expansion of local pullback solutions, whose behavior, when estimated well, is tied intimately to r-tipping. They again consider one dimensional systems, with the restriction that the system, while non-autonomous, is asymptotically autonomous.

Ritchie and Sieber attempt in [17] to define early warning signs for r-tipping using observational time series data, rather than a rigorous condition for existence or nonexistence of tipping. This more pragmatic approach shows that an increase of variance and an increase in autocorrelation, two usual early warning signals for tipping, are present but delayed in an archetypal model in which rate-induced tipping phenomena are found. Such early warning signs are useful in real-world systems where a simplified model is not necessarily useful or appropriate, and can be applied directly to real data. However, these signals fail to present any insight into the actual mechanisms of tipping beyond predicting their onset.

In more recent work, Wieczorek, Xie, and Ashwin consider multidimensional nonautonomous systems, again with the restriction that they are asymptotically autonomous [23]. So, for open subsets $U \subseteq \mathbb{R}^n, V \subseteq \mathbb{R}^d$ they have some

$$x_t = f(x, \Gamma(t)) \quad \text{with} \quad x \in U, t \in \mathbb{R} \tag{1.11}$$

for $\Gamma : \mathbb{R} \to V$, $f : U \times V \to \mathbb{R}^n$ and f a C^1-smooth vector field. The time dependence of $\Gamma(t)$ is restricted asymptotically, so some limits $\Gamma^{\pm} \in \mathbb{R}^d$ exist:

$$\Gamma(t) \to \Gamma^{\pm} \quad \text{as} \quad t \to \pm\infty. \tag{1.12}$$

This allows the system to be simplified into the future (and/or past) autonomous limit system

$$x_t = f(x, \Gamma^{\pm}). \tag{1.13}$$

In the case in which $\Gamma(t)$ has both future and past limits, it is called *bi-asymptotically* limited. To characterize r-tipping in this system, they employ the technique described in detail in [24], which involves augmenting the system with an additional dependent variable $s = g(t)$, with $g(t)$ constructed to ensure that the added dimension is a compact interval. The result is a compactified system on extended phase space, e.g. $U \times [-1, 1]$, on the boundaries $(U \times \{\pm 1\})$ of which the autonomous dynamics of the future and past limits described above are preserved. Crucially, compact invariant sets from the limit systems, most usefully equilibria and invariant manifolds, can be used to study the nonautonomous system.

This method employs an analogous idea of using heteroclinic orbits to characterize r-tipping to that which was effective in our prototypical example (eq. (1.1), fig. 1.1). This is a powerful technique, as there are well developed continuation methods available which make computing such orbits accessible, bridging the gap between rigorous but in some cases impractical tipping criteria and purely statistical or computational methods.

Up to this point, we have considered rate-induced tipping in ODE models, and there is the natural question of what might happen to these phenomena in PDE models, with the addition of spatial dynamics. Hasan, Mac Cárthaigh, and Wieczorek study r-tipping in nonautonomous asymptotically homogeneous reaction diffusion equations (RDEs) in one spatial dimension [7]. They consider the full system

$$u_t = du_{xx} + f(u, H(x - ct))$$

for $x \in \mathbb{R}$ spatial coordinate, t time, d the diffusion coefficient, reaction term f, and shift rate c. Dirichlet boundary conditions are imposed on the unbounded domain, so $\lim_{x \to \pm\infty} u(x, t) = u^{\pm} \in \mathbb{R}$. They are specifically considering an application to population

dynamics, so here $H(x-ct)$ is a 'habitat' function which is C^1-smooth and asymptotically autonomous (i.e. $H(x-ct) \to h^{\pm}$ as $t \to \infty$).

Exploiting the reaction term's linear dependence on time, this system can be reformulated to a so called moving-frame ODE with the coordinate change $\xi = x - ct$. Then, after appropriate nondimesnionalization of the model, the same general approach as outlined before is taken: the system is compactified (e.g. with the technique in [23]), and heteroclinic orbits in the compactified system are numerically investigated (e.g. with Lin's method [11] in this particular paper, although any suitable numerical method for computing these orbits could be employed). Both b-tipping and r-tipping effects are observed in their system, and continuing study of this and other spatially extended systems with r-tipping presents a rich opportunity for broadening understandings of r-tipping in diverse contexts.

1.2 Interaction with other tipping modes

While much of the literature discussed so far focuses on prototypical models of rate-induced tipping in which other tipping effects are either not present or not discussed, r-tipping can coexist with other tipping modes, and may even create novel effects in interactions with these modes.

In particular, noise- and rate-induced tipping are natural to consider together given that both are very often components of models describing real-world phenomena [20]. Slyman and Jones were able to determine that the addition of noise to a one-dimensional system displaying rate-induced tipping enabled tipping below the expected critical rate, and at a higher probability of occurring than expected for exclusively noise induced tipping. So, in some sense these two mechanisms provide positive feedback to each other, enabling tipping where it would not otherwise be expected to be present in either mode alone.

Rate-induced tipping may also interact with bifurcation induced tipping. Cantisán characterizes various rate and memory effects which are present in systems with a drifting parameter which undergo bifurcation induced tipping [3].

The beauty and the difficulty of these phenomena lie in their complexity; endless combinations of effects are possible, with properties as wide ranging as the applications which inspire this work in the first place.

1.3 Applications

Beyond being interesting mathematical problems, rate-induced tipping effects are found in applications ranging from fire ecology [14] to epidemiology [13], [12].

Merker and Kunsch take the recent global pandemic as a rich context in which to investigate r-tipping, asking if not only the level of lockdown restrictions, but the rate at which they were implemented, may have had critical effects on the transmission of disease [13], [12]. Consider the pandemic response in the United States– different states implemented similar lockdown policies, but at different rates. It turns out that in a non-smooth epidemiological model, two model states taking identical measures at identical times may have drastically different outcomes– eradication of disease versus the disease becoming endemic– based solely on a differing *rate* of implementation.

In this case, policy implementation– though in reality a nuanced issue with among other things institutional inertia and political concerns as confounding factors– happens at a rate that can ultimately be dictated by government officials and policymakers. But where Merker and Kunsch have a directly manipulable rate, other systems may not be so easy to control. Rising global temperature is one such example. While a factor in many models, e.g. high dimensional mutualistic plant-pollinator networks [15], rate of warming is difficult to directly tune. Investigating this model, Panahi et al. [15] find that probability of r-tipping saturates rapidly as rate increases, meaning that reducing chances of tipping meaningfully requires reducing the rate itself to near zero. This has serious implications for climate affected systems, where taking measures to reduce the rate of warming has proven to be an enormously challenging political issue.

The largest source of global carbon emissions is human usage of fossil fuels, but release of carbon from wildfires and permafrost thaw is also an important factor in global emissions. In peatlands, which are crucial global carbon sinks, a rather strange phenomenon of 'zombie' fires has been observed, in which fires appear to be extinguished, yet reemerge from the soil after the winter season has passed. O'Sullivan et al. propose rate-induced tipping as a possible mechanism for this behavior, which previously was not well understood [14]. They use the compactification strategy previously discussed in section 1.1 ([1], [24], [23], [7]), and find that a rate-induced tipping event can happen in physically and ecologically relevant parameter ranges which tip the modeled soil system into a hot metastable state. This state is consistent with the observed zombie fires, is triggered by a rather modest rate of global warming, and persists for a period of up to a decade.

The persistence of this hot metastable state is a critical issue– peatlands burned in this manner for such an extended period are a significant loss to global carbon stores and may have a catastrophic cascading effect on global temperature rise. As peatlands burn and release carbon into the atmosphere, this new carbon compounds greenhouse effects in a positive feedback loop, creating even more favorable conditions for wildfires.

As discussed in section 1.2, tipping effects in general do not exist in isolation. In a model of a tropical cyclone noise and rate-induced tipping effects can be observed in concert [21]. While their contributions individually in this model have been investigated, their interaction has not, and presents an opportunity for further study.

Looking ahead

The breadth of applications in which tipping phenomena are observed provides motivation to discover and characterize not-yet understood tipping modes. Rate-induced tipping is a burgeoning area of research, with both theoretical lines of questioning and applications waiting to be explored. Much has been developed for r-tipping in prototypical cases, but less well understood are the more complicated interactions with other tipping modes, or effects in spatially coupled systems, the latter of which is the focus of the following chapter. The wide ranging implications of these effects in real-world systems make this a compelling problem, and there is room for meaningful contributions in both applied settings and in the theoretical canon.

Chapter 2

Understanding reverse tipping

Here we study rate-induced tipping and related effects in a spatially extended system. We consider the dynamics of a nonlinear reaction diffusion equation in one spatial dimension, as in the work previously discussed, by Hasan et. al. [7]. However, rather than considering a reaction term particularly tailored to the application of habitat and population growth, we choose a simple reaction term supporting a bistability– similar to what we had in our expository example of r-tipping in section 1.1.

To illustrate the phenomenon hereafter discussed, consider a bistable ecosystem with both forest and prairie biomes supported, and diffusion across their boundary. Suppose, given some stable balance of forest and prairie makeup, there is some disturbance to this balance in space and time– e.g. shifting climate zones due to climate change or some other global factor. This perturbation, propagating at a fixed speed, favors one or the other of the habitats. Say this perturbation is an invasion of a warmer climate zone, which favors the prairie biome. Thus as this invading front progresses spatio-temporally we would expect a 'tipping' from forest to prairie at the boundary of this front. What we can see, quite dramatically, is that if this front invades at a high enough speed, the diffusion in the system actually causes a kind of 'tipping' cascade which can precede the tipping front itself!

This 'reverse tipping' is characterized by a secondary tipping front propagating *ahead* of the front that is progressing spatially. So, in our example, one would find prairie dominance beyond the invading climate zone where it is expected (see fig. 2.1). This is an unexpected and quite interesting result, which the rest of this chapter is devoted to describing.

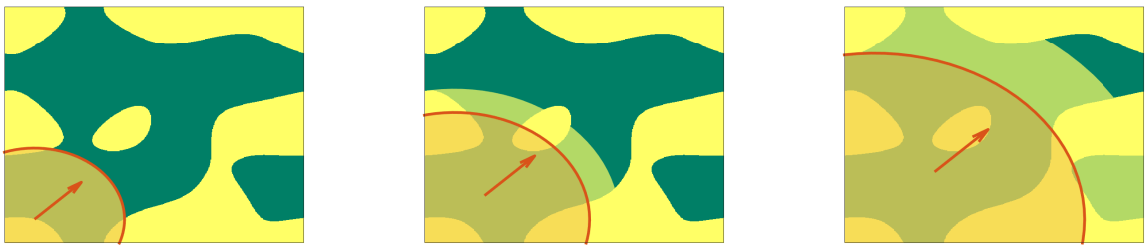

Figure 2.1: Reverse tipping in action: prairie invasion (yellow) of forest (green) ahead of invading climate zone front (red).

2.1 System set up

We consider the following system

$$u_t = du_{xx} + f(u - \mu) \tag{2.1}$$

with diffusion coefficient d and parameter μ. We take f as the simple bistable system

$$f(u) = u(1-u)(u-a) \tag{2.2}$$

for $0 < a < 1$. The equilibria of f are $u_- = 0, u_+ = 1$, and $u_\circ = a$. The upper and lower states u_- and u_+ are stable, and the middle state $u_\circ$ is unstable. Our parameter μ is changing, and we model this by letting it be a function of space and time

$$\mu(x,t) = \chi(x - ct) \tag{2.3}$$

for some 'tipping profile' χ that propagates spatially at rate c. For χ monotonely decreasing from M to 0 (χ a hyperbolic tangent function, for instance), we have μ going from M to 0 at a rate determined by the profile of χ. It is convenient to convert to the corresponding moving frame ODE using the change in coordinates $x - ct \to \xi$, under which the profile χ evolves according to

$$\chi_\xi = -\varrho\chi(\xi)(M - \chi(\xi)) \tag{2.4}$$

where the rate of change of μ from M to 0 is determined by ϱ. In the limit $\varrho \to +\infty$ this change is instantaneous. Converting the full system to the moving frame coordinate ξ (and choosing to encode spatial coupling strength d within ϱ and c by rescaling $\tilde{c} = \frac{c}{\sqrt{d}}$, $\tilde{\varrho} = \varrho\sqrt{d}$ rather than maintaining the coefficient) we have

$$u_t(\xi) = u_{\xi\xi} + cu_\xi + f(u - \chi(\xi)). \tag{2.5}$$

Now, to understand the quasi-stable states in the original systems we can simply consider stationary states in the moving frame system

$$0 = u_{\xi\xi} + cu_\xi + f(u - \chi(\xi)) \tag{2.6}$$

$$\chi_\xi = -\varrho\chi(\xi)(M - \chi(\xi)) \tag{2.7}$$

Introducing a dummy variable $u_\xi = v$ gives the three dimensional ODE system

$$u_\xi = v \tag{2.8}$$

$$v_\xi = -cv - f(u - \chi(\xi)) \tag{2.9}$$

$$\chi_\xi = -\varrho\chi(\xi)(M - \chi(\xi)) \tag{2.10}$$

Thus we have equilibria $(u_\star, v_\star, \chi_\star)$ for $v_\star = 0$, $\chi_\star = 0, M$, and $u_\star = u_{-,\circ,+} + \chi_\star$ for lower, middle, and upper equilibria of f ($u_-, u_\circ$, and u_+) respectively.

Our aim is to understand these equilibria in the moving frame, and exploit the explicit asymptotic dynamics $\chi(\xi) \to \chi^\pm = 0, M$ for $t \to \pm\infty$. We do this by analyzing the $u - v$ planar phase portrait geometry at $\chi^\pm$, rather than taking the more traditional approach of direct simulation to characterize the existence and onset of this phenomenon. In the limit of $\varrho \to +\infty$, this analysis is exact, and it can be extended, with some correction, to ϱ finite, although that extension is not the focus of this work.

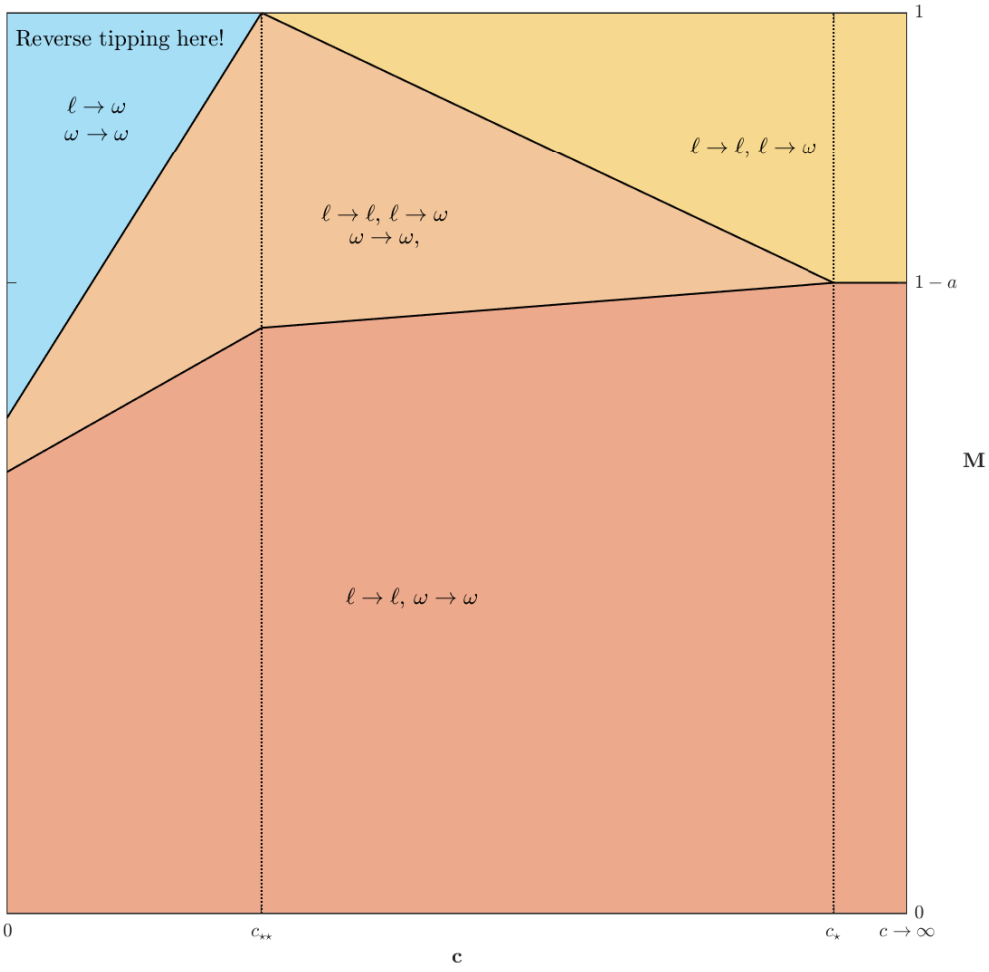

Figure 2.2: Sketch of phase transitions characteristic in this system. Reverse tipping is restricted to low c (corresponding, in this limit $\varrho \to +\infty$, to high strength of spatial coupling. Colored regions are characterized by the existence of monotone heteroclinic trajectories (labeled according to the equilibria they connect: ℓ for lower, ω for upper). The following sections detail critical values $c_\star$ (section 2.2.2)and $c_{\star\star}$ (section 2.2.3) and the mechanisms by which they occur. See section 2.2.4 for full discussion of these different regimes.

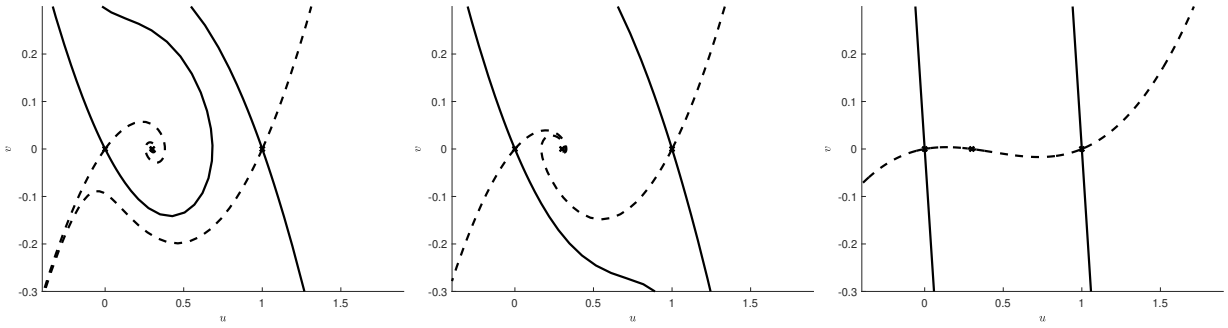

(a) $0 < c < c_{\star\star}$ (b) $c_{\star\star} < c < c_{\star}$ (c) $c_{\star} < c$

Figure 2.3: Phase portraits visualized as stable (solid) and unstable (dashed) invariant manifolds of u_+, u_- equilibria for a choice of a, in order of increasing c.

2.2 The limit $\varrho = +\infty$

Fixing $0 < a < \frac{1}{2}$, in the $\varrho \to +\infty$ limit, we split into three regimes of speed c, where the relevant phase portraits in the $u - v$ plane for $\chi_\xi = 0$ are qualitatively different (fig. 2.3). We have the case of large c (fig. 2.3c), which essentially reduces to a one dimensional case, and the two relatively more interesting regimes ($fig.$ 2.3a and $fig.$ 2.3b) for moderate-to-low speeds c.

Choice of a does not influence the existence of these regimes, although it does change their onset and the mechanism by which certain regime shifts occur, and the orientation of the phase portrait (choices of $\frac{1}{2} < a < 1$ produce 180° rotations of the corresponding $0 < 1 - a < \frac{1}{2}$ portrait). The critical values which divide these regimes, called $c_\star$ and $c_{\star\star}$, can be explicitly calculated for a given a.

As previously discussed, the existence of tipping states can be characterized by heteroclinic orbits– intersections in stable and unstable invariant manifolds of appropriate equilibria. Conveniently, in this limit, we can find these intersections geometrically by simply overlaying the phase portraits of the asymptotic dynamics at $\chi_\star = 0$ and $\chi_\star = M$ (which are simply translates of each other, by exactly M). These heteroclinic trajectories are classified by the equilibria they originate from (at $t = -\infty$) and their terminus for $t = +\infty$. We use ℓ to identify the lower equilibria, and ω to identify the upper. A trajectory $\ell \to \omega$ would thus indicate a monotone heteroclinic trajectory connecting the lower equilibria at $-\infty$ to the upper at $+\infty$.

2.2.1 For high speeds c

In this $\varrho \to +\infty$ limit, spatial coupling is encoded in speed of propagation of the μ tipping profile– increasing speed effectively reduces spatial coupling (recall the scaling $\tilde{c} = \frac{c}{\sqrt{d}}$ from section 2.1). For c very large, the phase space approaches the degenerate case with an infinite line of equilibria along $v = 0$ and infinitely many parallel half line solutions approaching them. In the perfect one dimensional case the only possible intersections of the stable with the unstable invariant manifolds are the coincidence of the equilibria themselves. For c large, but still finite, there are only slight deviations from the limiting case (fig. 2.7).

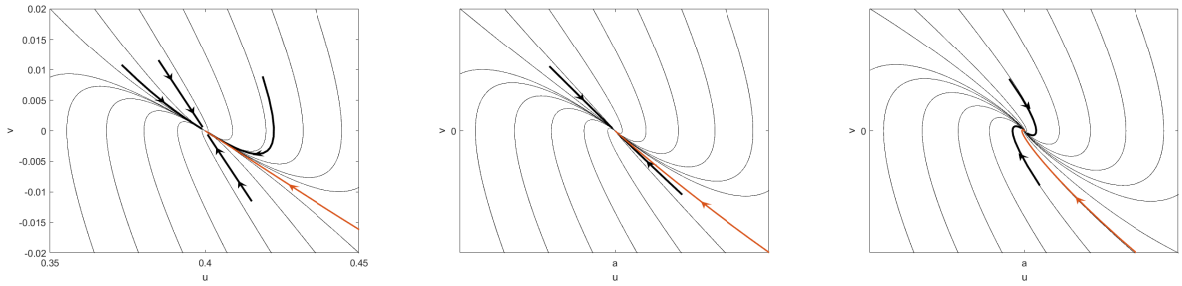

(a) $c > c_\star$ (b) $c = c_\star$ (c) $c < c_\star$

Figure 2.4: Local phase space about $u_\circ$ as around $c = c_\star$, when $\frac{1}{3} < a < \frac{1}{2}$. Stable manifolds of $u_\circ$ in black, unstable manifold of u_+ shown in red.

2.2.2 Critical $c_\star$: appearance of non-monotone trajectories

The first important qualitative change in the $u - v$ phase portrait for decreasing c occurs when the unstable invariant manifolds start to twist about the middle equilibrium– introducing a possibility for non-monotone trajectories (fig. 2.3b). This happens by two distinct mechanisms for $0 < a < \frac{1}{3}$ and $\frac{1}{3} < a < \frac{1}{2}$. The first mechanism (occuring at $c_{\star,1}$) is perhaps the more expected, corresponding to the degeneration of the eigenspace of the middle equilibria that we would classically expect to cause a transition between sink and spiral sink, when the eigenvalues of the linearization gain nonzero complex part. The second occurs when there is an intersection between the strongly stable invariant manifold of the middle equilibrium and the unstable invariant manifold of the upper, after which the unstable invariant manifold 'crosses over' the strongly stable manifold and curls around to approach the middle equilibrium from the other side.

The node-to-focus transition, $\frac{1}{3} < a < \frac{1}{2}$

Since the critical value $c_{\star,1}$ occurs when we have degenerate eigenvalues in the linearization of the system, we can rather straightforwardly compute its onset. Here, we disregard the distinction between the $\chi = 0$ and $\chi = M$ cases as the $u - v$ plane is identical up to translation at these extrema. We can, in fact, reduce to the two dimensional system

$$u_\xi = v \tag{2.11}$$
$$v_\xi = -cv - f(u) \tag{2.12}$$

with corresponding Jacobian

$$\begin{pmatrix} 0 & 1 \\ -\frac{\delta}{\delta u} f(u) & -c \end{pmatrix} \quad @(u = a) : \begin{pmatrix} 0 & 1 \\ a^2 - a & -c \end{pmatrix}. \tag{2.13}$$

This gives eigenvalues

$$\lambda_{1,2} = \frac{1}{2}\left(\pm\sqrt{4(a^2 - a) + c^2} - c\right) \tag{2.14}$$

with the degenerate double eigenvalue case occurring when

$$4(a^2 - a) + c^2 = 0 \implies c_\star = 2\sqrt{a - a^2}. \tag{2.15}$$

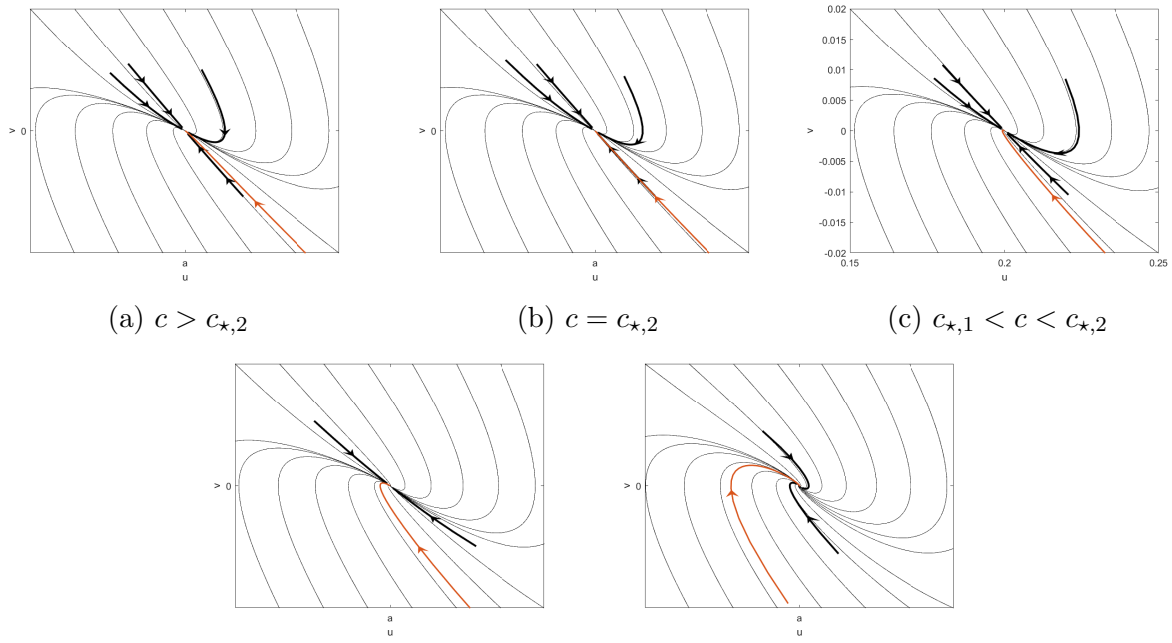

(a) $c > c_{\star,2}$ (b) $c = c_{\star,2}$ (c) $c_{\star,1} < c < c_{\star,2}$

(d) $c = c_{\star,1}$ (e) $c < c_{\star,1}$

Figure 2.5: Local phase space about $u_\circ$ around $c = c_{\star,2}$ and then $c = c_{\star,1}$, for when $0 < a < \frac{1}{3}$. Stable manifolds of $u_\circ$ in black, unstable manifold of u_+ shown in red. Compare fig. 2.5d, fig. 2.5e to the $a > \frac{1}{3}$ case in fig. 2.4

Note that this is well defined, as $0 < a < 1$ guarantees $a^2 < a$. This double eigenvalue corresponds to a degenerate case, where the vector field *just* begins to rotate around the middle equilibrium. For values $0 < c < c_{\star,1}$ the eigenvalues become complex and we get a logarithmic spiral (fig. 2.4).

This transition certainly occurs for *all* a, but is superseded by the mechanism described below when $a < \frac{1}{3}$.

Pass-through of strong stable manifold, $a < \frac{1}{3}$

For $a < 1/3$ there is another critical $c_{\star,2}$ occuring where the unstable manifold of the upper equilibrium passes through the strongly stable manifold of the middle equilibrium, occuring *before* the eigenspace degenerates at $c_{\star,1}$. We can compute this value of $c_{\star,2}$ explicitly, owing to the nonlinearity f being cubic. The relevant heteroclinic orbit then turns out to be a parabola. Using the ansatz

$$v = \alpha(u - a)(1 - u) \tag{2.16}$$

we have

$$v_\xi = -\alpha(u - a)u_\xi + \alpha(1 - u)u_\xi. \tag{2.17}$$

Substituting our expression for $v(u)$ (eq. (2.16), using the fact that $u_\xi = v$) into eq. (2.17), we then have two expressions v, v_ξ in terms of u, and can substitute these into our original

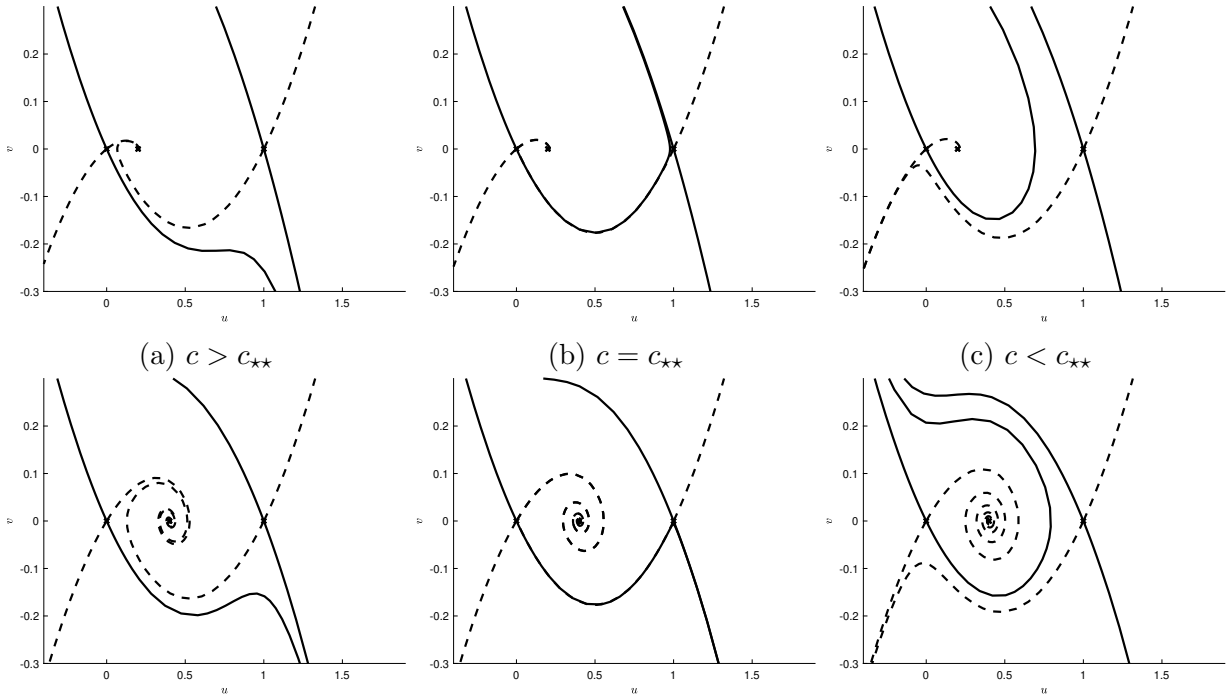

(a) $c > c_{\star\star}$ (b) $c = c_{\star\star}$ (c) $c < c_{\star\star}$

(d) $c > c_{\star\star}$ (e) $c = c_{\star\star}$ (f) $c < c_{\star\star}$

Figure 2.6: Phase space in $u - v$ plane around $c = c_{\star\star}$, for $0 < a < \frac{1}{3}$ (a-c) and $\frac{1}{3} < a < \frac{1}{2}$ (d-f).

system (eq. (2.12)). Gathering coefficients for each order u we obtain the system

$$2\alpha^2 - 1 = 0 \tag{2.18}$$

$$-a^2\alpha^2 - a\alpha^2 - ca\alpha = 0 \tag{2.19}$$

which gives $\alpha = \frac{1}{\pm\sqrt{2}}$ (the α positive case leads to $c < 0$, so we discard this solution). We have

$$-\frac{1}{2}a^2 - \frac{1}{2}a - ca\frac{1}{-\sqrt{2}} = 0 \implies c_{\star,2} = \frac{a+1}{\sqrt{2}}. \tag{2.20}$$

Note that $c_{\star,2} \geq c_{\star,1}$ for all a, and $c_{\star,2} = c_{\star,1}$ precisely for $a = \frac{1}{3}$.

2.2.3 Critical $c_{\star\star}$: wrapping of stable invariant manifold

The second important qualitative change in the $u - v$ phase portrait occurs when the stable manifold of the lower equilibrium begins to wrap around the middle equilibrium (fig. 2.6). The point at which this occurs is another heteroclinic orbit, this time connecting the lower equilibrium with the upper. We follow the same procedure as above to explicitly calculate $c_{\star\star}$, with the ansatz

$$v = \beta u(1 - u). \tag{2.21}$$

Again substituting $v(u)$, $v_\xi(u)$ to obtain an expression of powers of u and gathering coefficients gives $\beta = -\frac{1}{\sqrt{2}}$, and $c_{\star\star} = \sqrt{2} \cdot (\frac{1}{2} - a)$

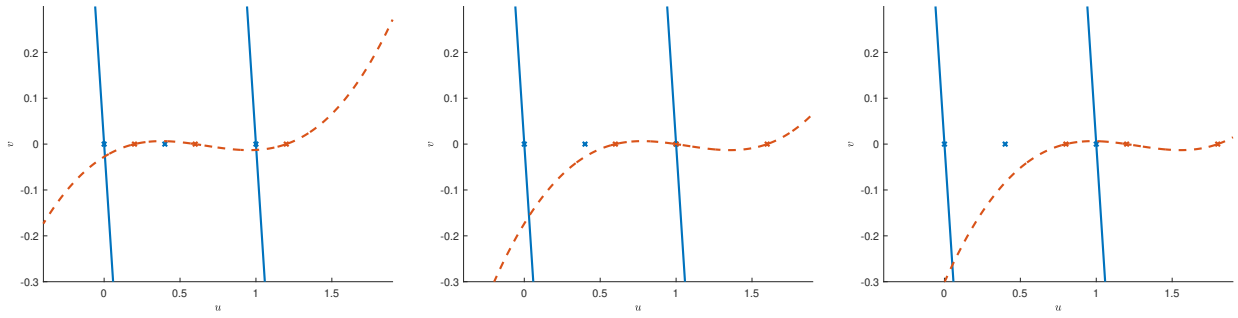

(a) $M < 1-a$. Only $\ell \to \ell$ and $\omega \to \omega$ states are stable.

(b) $M = 1 - a$

(c) $M > 1-a$. Only the $\ell \to \ell$ and $\ell \to \omega$ states are stable.

Figure 2.7: Cases for $c > c_\star$.

2.2.4 Discussion

Now we investigate the planar phase portraits in each of these three relevant regimes of c. Relevant trajectories are indicated by intersections between the unstable invariant manifolds of the equilibria at $(u_\star, v_\star, M)$ (red in the following figures), and the stable invariant manifolds of the equilibria at $(u_\star, v_\star, 0)$ (blue in the following figures). For a choice of c within the relevant range, we can identify critical values of M at which such intersections appear or disappear, indicating the creation or destruction of a stable trajectory.

Large $c > c_\star$

First, consider the case $c > c_\star$, where the dynamics approach the one dimensional case. See fig. 2.2 again for a visual representation of these regimes. As shown in fig. 2.7a, for $M < 1 - a$ only $\ell \to \ell$ and $\omega \to \omega$ states are present. For $M > 1 - a$, there are only $\ell \to \ell$ and $\ell \to \omega$ states– the unstable invariant manifold of the upper equilibrium has no intersections with the stable invariant manifolds of the other equilibria (fig. 2.7c).

Moderate $c_{\star\star} < c < c_\star$

The same three monotone trajectories ($\ell \to \ell$, $\ell \to \omega$, and $\omega \to \omega$) are present certain regimes of M as for $c > c_\star$. However, where previously the creation of the tipping state $\ell \to \omega$ coincides with the destruction of the stable, non-tipping $\omega \to \omega$ state, here those states can coexist for an intermediate range of M (fig. 2.8).

Neither of these first two c regimes display the reverse tipping phenomena we are looking for– when $\omega \to \omega$ loses stability, it tips to the $\ell \to \omega$ state, which happens behind the tipping front. So, let us turn to the final case $0 < c < c_{\star\star}$.

Small $c < c_{\star\star}$

Here we have our reverse tipping! When M is large enough that the $\ell \to \ell$ state is no longer stable, we observe a tipping to the $\ell \to \omega$ state. That tipping from $\ell \to \omega$ occurs *ahead* of the μ tipping front propagating at speed c (so, faster than the moving QSE), as seen in fig. 2.10. This shows that strong spatial coupling can effectively pull a solution back from tracking a QSE as it passes a tipping threshold, and this 'pulling back' can cascade through the system at a rate *above* the propagation speed of the original tipping, causing it to *precede* to original effect. That is quite an unexpected phenomenon.

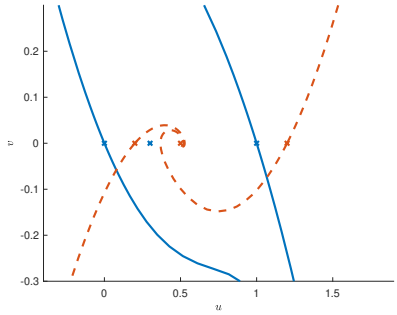

(a) Only non-tipping states $\ell \to \ell$ and $\omega \to \omega$ states are stable.

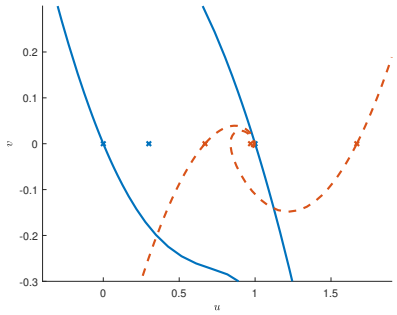

(b) A tangency occurs at which a new intersection representing a monotone trajectory $\ell \to \omega$ is created.

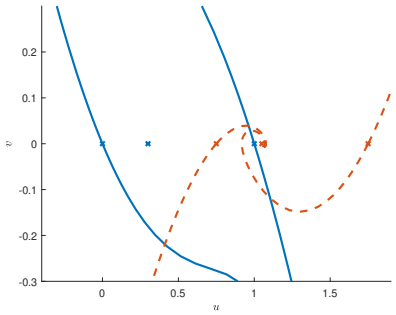

(c) The new tipping state $\ell \to \omega$ coexists with the non-tipping $\ell \to \ell$ and $\omega \to \omega$ states.

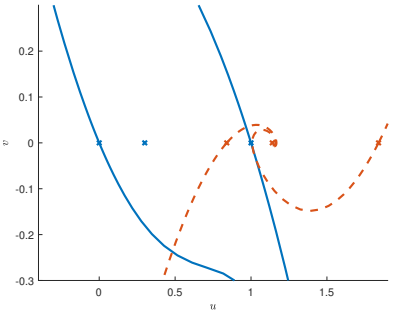

(d) A tangency occurs after which the $\omega \to \omega$ trajectory is destroyed.

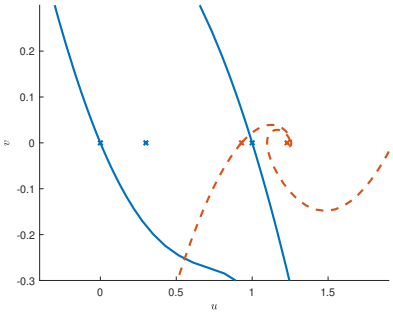

(e) Only the $\ell \to \ell$ and $\ell \to \omega$ states persist.

Figure 2.8: Cases for $c_{\star\star} < c < c_{\star}$

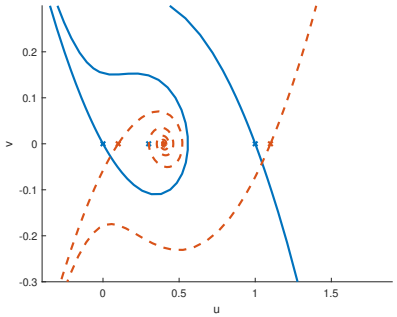

(a) Initially only the non-tipping states $\ell \to \ell$ and $\omega \to \omega$ are stable.

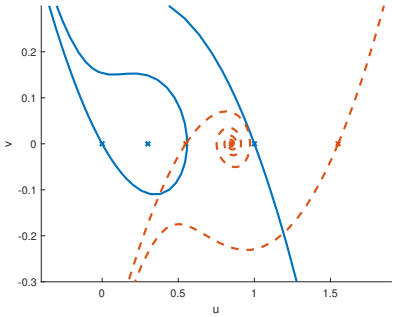

(b) For a range of M, all three states $\ell \to \ell$, $\ell \to \omega$, and $\omega \to \omega$ are stable.

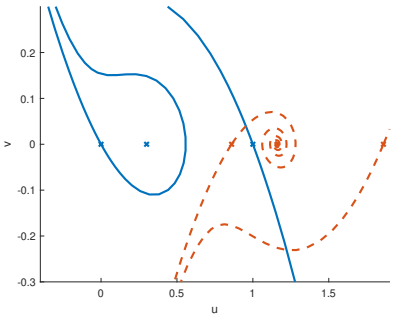

(c) Only the $\ell \to \omega$ and $\omega \to \omega$ states persist.

Figure 2.9: Cases for $c < c_{\star\star}$

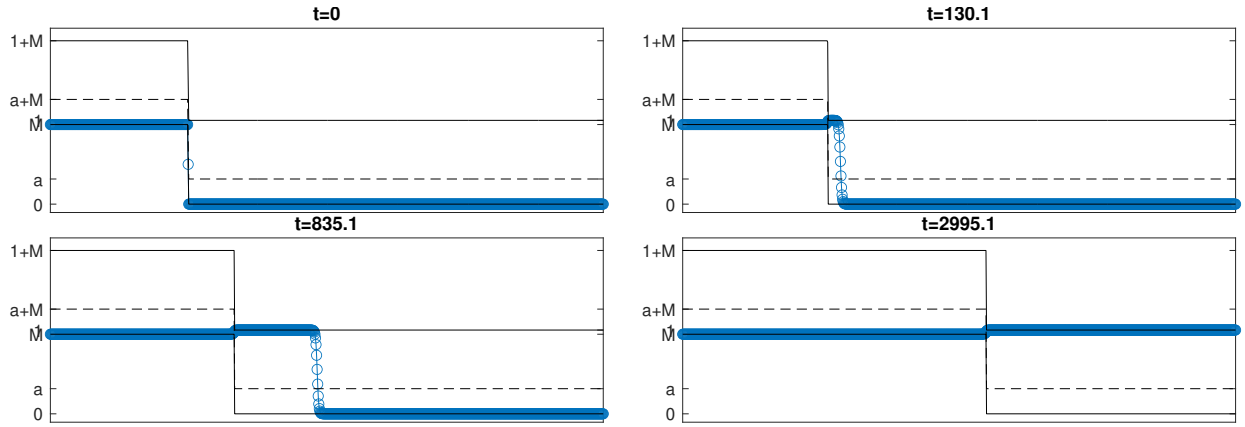

Figure 2.10: Reverse tipping phenomenon observed for M large– tipping front propagates *ahead* of spatial tipping due of μ.

As it turns out, $c_{\star\star}$ is the threshold below which reverse tipping occurs. This effect only occurring for c small makes sense, given that it in some sense requires spatial coupling strength to 'overcome' the solution's natural desire to track the quasi-stable equilibrium across the change in parameter μ.

In direct simulation, in a system extended in one spatial dimension, the reverse tipping phenomenon is shown here. It propagates ahead of the spreading speed of the system, so as $t \to \infty$ it reaches the $\ell \to \omega$ state.

2.3 Future work

The focus of this work has been to contextualize the reverse tipping phenomenon within the non-classical tipping landscape, and then to characterize it, choosing a convenient limiting regime. While this phenomenon has been observed in direct numerical simulations to exist for finite ϱ, rigorous analysis to prove its existence remains to be done. There is more to be precisely understood about the phenomena itself as well– such as exactly how much faster than the original tipping front the reverse tipping front propagates.

In addition, given the relevance to applications, exploring this phenomenon within specific models also presents an opportunity for future work. Non-classical tipping effects like reverse tipping are still relatively poorly understood. Exploring reverse tipping in relation to other non-classical tipping effects will help to expand the tipping theory established by classical bifurcation theory.

Bibliography

[1] Peter Ashwin, Clare Perryman, and Sebastian Wieczorek. "Parameter shifts for nonautonomous systems in low dimension: Bifurcation- and Rate-induced tipping". In: *Nonlinearity* 30.6 (June 2017). arXiv:1506.07734 [math], pp. 2185–2210. ISSN: 0951-7715, 1361-6544. DOI: 10.1088/1361-6544/aa675b. URL: http://arxiv.org/abs/1506.07734 (visited on 12/16/2024).

[2] Peter Ashwin et al. "Tipping points in open systems: bifurcation, noise-induced and rate-dependent examples in the climate system". In: *Philosophical Transactions of the Royal Society A: Mathematical, Physical and Engineering Sciences* 370.1962 (Mar. 2012), pp. 1166–1184. DOI: 10.1098/rsta.2011.0306. URL: https://royalsocietypublishing.org/doi/full/10.1098/rsta.2011.0306 (visited on 10/30/2024).

[3] Julia Cantisán et al. "Rate and memory effects in bifurcation-induced tipping". In: *Physical Review E* 108.2 (Aug. 2023), p. 024203. DOI: 10.1103/PhysRevE.108.024203. URL: https://link.aps.org/doi/10.1103/PhysRevE.108.024203 (visited on 11/12/2024).

[4] Peter Ditlevsen. "Tipping points in the climate system". In: *Nonlinear and stochastic climate dynamics*. Cambridge Univ. Press, Cambridge, 2017, pp. 33–53. ISBN: 9781107118140.

[5] Eric Forgoston and Richard O. Moore. "A Primer on Noise-Induced Transitions in Applied Dynamical Systems". In: *SIAM Review* 60.4 (Jan. 2018), pp. 969–1009. ISSN: 0036-1445. DOI: 10.1137/17M1142028. URL: https://epubs.siam.org/doi/10.1137/17M1142028 (visited on 12/03/2024).

[6] Jonathan Hahn. "Rate-Dependent Bifurcations and Isolating Blocks in Nonautonomous Systems". en. In: (Sept. 2017). URL: https://hdl.handle.net/11299/192674 (visited on 12/15/2024).

[7] Cris R. Hasan, Ruaidhrí Mac Cárthaigh, and Sebastian Wieczorek. "Rate-Induced Tipping in Heterogeneous Reaction-Diffusion Systems: An Invariant Manifold Framework and Geographically Shifting Ecosystems". In: *SIAM Journal on Applied Dynamical Systems* 22.4 (Dec. 2023), pp. 2991–3024. DOI: 10.1137/22M1536625. URL: https://epubs.siam.org/doi/full/10.1137/22M1536625 (visited on 09/18/2024).

[8] Claire Kiers and Christopher K. R. T. Jones. "On Conditions for Rate-induced Tipping in Multi-dimensional Dynamical Systems". en. In: *Journal of Dynamics and Differential Equations* 32.1 (Mar. 2020), pp. 483–503. ISSN: 1572-9222. DOI: 10.1007/s10884-019-09730-9. URL: https://doi.org/10.1007/s10884-019-09730-9 (visited on 12/15/2024).

[9] Christian Kuehn and Iacopo P. Longo. "Estimating rate-induced tipping via asymptotic series and a Melnikov-like method*". en. In: *Nonlinearity* 35.5 (May 2022), p. 2559. ISSN: 0951-7715. DOI: 10.1088/1361-6544/ac62dc. URL: https://dx.doi.org/10.1088/1361-6544/ac62dc (visited on 11/12/2024).

[10] Timothy M. Lenton et al. "Tipping elements in the Earth's climate system". In: *Proceedings of the National Academy of Sciences* 105.6 (Feb. 2008), pp. 1786–1793. DOI: 10.1073/pnas.0705414105. URL: https://www.pnas.org/doi/10.1073/pnas.0705414105 (visited on 12/15/2024).

[11] Xiao-Biao Lin. "Using Melnikov's method to solve Silnikov's problems". In: *Proceedings of the Royal Society of Edinburgh Section A: Mathematics* 116.3-4 (Nov. 1990), pp. 295–325. DOI: https://doi.org/10.1017/S0308210500031528. URL: https://www.cambridge.org/core/journals/proceedings-of-the-royal-society-of-edinburgh-section-a-mathematics/article/abs/using-melnikovs-method-to-solve-silnikovs-problems/C651F17B29C54D6FD72EF8FC6E2965DD.

[12] Jochen Merker. "Rate-Induced Tipping and Chaos in Models of Epidemics". en. In: ed. by Carla M.A. Pinto and Clara Mihaela Ionescu. Cham: Springer Nature Switzerland, 2023, pp. 85–102. ISBN: 9783031426896. DOI: 10.1007/978-3-031-42689-6_4. URL: https://doi.org/10.1007/978-3-031-42689-6_4 (visited on 11/12/2024).

[13] Jochen Merker and Benjamin Kunsch. "Rate-Induced Tipping Phenomena in Compartment Models of Epidemics". en. In: ed. by Praveen Agarwal et al. Singapore: Springer, 2021, pp. 307–328. ISBN: 9789811624506. DOI: 10.1007/978-981-16-2450-6_14. URL: https://doi.org/10.1007/978-981-16-2450-6_14 (visited on 11/12/2024).

[14] Eoin O'Sullivan, Kieran Mulchrone, and Sebastian Wieczorek. "Rate-induced tipping to metastable Zombie fires". In: *Proceedings of the Royal Society A: Mathematical, Physical and Engineering Sciences* 479.2275 (July 2023), p. 20220647. DOI: 10.1098/rspa.2022.0647. URL: https://royalsocietypublishing.org/doi/10.1098/rspa.2022.0647 (visited on 11/12/2024).

[15] Shirin Panahi et al. "Rate-induced tipping in complex high-dimensional ecological networks". In: *Proceedings of the National Academy of Sciences* 120.51 (Dec. 2023), e2308820120. DOI: 10.1073/pnas.2308820120. URL: https://www.pnas.org/doi/10.1073/pnas.2308820120 (visited on 11/12/2024).

[16] H. Poincaré. "Sur l'équilibre d'une masse fluide animée d'un mouvement de rotation". en. In: *Acta Mathematica* 7.0 (Jan. 1885), pp. 259–380. ISSN: 0001-5962. DOI: 10.1007/BF02402204. URL: http://projecteuclid.org/euclid.acta/1485888300 (visited on 12/03/2024).

[17] Paul Ritchie and Jan Sieber. "Early-warning indicators for rate-induced tipping". In: *Chaos: An Interdisciplinary Journal of Nonlinear Science* 26.9 (Sept. 2016), p. 093116. ISSN: 1054-1500. DOI: 10.1063/1.4963012. URL: https://doi.org/10.1063/1.4963012 (visited on 12/15/2024).

[18] Arnd Scheel. *Lecture notes in dynamical systems and differential equations*. University of Minnesota. 2018.

[19] Marten Scheffer. *Critical Transitions in Nature and Society*. la. Google-Books-ID: okT_DwAAQBAJ. Princeton University Press, Nov. 2020. ISBN: 9781400833276.

[20] Katherine Slyman and Christopher K. Jones. "Rate and noise-induced tipping working in concert". In: *Chaos: An Interdisciplinary Journal of Nonlinear Science* 33.1 (Jan. 2023), p. 013119. ISSN: 1054-1500. DOI: 10.1063/5.0129341. URL: https://doi.org/10.1063/5.0129341 (visited on 11/12/2024).

[21] Katherine Slyman et al. "Tipping in a low-dimensional model of a tropical cyclone". In: *Physica D: Nonlinear Phenomena* 457 (Jan. 2024), p. 133969. ISSN: 0167-2789. DOI: 10.1016/j.physd.2023.133969. URL: https://www.sciencedirect.com/science/article/pii/S0167278923003238 (visited on 11/12/2024).

[22] S. Wieczorek et al. "Excitability in ramped systems: the compost-bomb instability". In: *Proceedings of the Royal Society A: Mathematical, Physical and Engineering Sciences* 467.2129 (Nov. 2010), pp. 1243–1269. DOI: 10.1098/rspa.2010.0485. URL: https://royalsocietypublishing.org/doi/10.1098/rspa.2010.0485 (visited on 12/03/2024).

[23] Sebastian Wieczorek, Chun Xie, and Peter Ashwin. "Rate-induced tipping: thresholds, edge states and connecting orbits". en. In: *Nonlinearity* 36.6 (May 2023), p. 3238. ISSN: 0951-7715. DOI: 10.1088/1361-6544/accb37. URL: https://dx.doi.org/10.1088/1361-6544/accb37 (visited on 10/30/2024).

[24] Sebastian Wieczorek, Chun Xie, and Chris K. R. T. Jones. "Compactification for asymptotically autonomous dynamical systems: theory, applications and invariant manifolds". en. In: *Nonlinearity* 34.5 (May 2021), p. 2970. ISSN: 0951-7715. DOI: 10.1088/1361-6544/abe456. URL: https://dx.doi.org/10.1088/1361-6544/abe456 (visited on 12/03/2024).